Science in One Health 3 (2024) 100068

Contents lists available at ScienceDirect

Science in One Health

journal homepage: www.journals.elsevier.com/science-in-one-health

Full length article

Identification of habitat suitability for the dominant zoonotic tick species *Haemaphysalis flava* on Chongming Island, China

Si-Wei Fei [a,1], Han-Qing Zhao [a], Jing-Xian Yin [a], Zhi-Shan Sun [a], Jing-Bo Xue [b], Shan Lv [b], Xin-Yu Feng [a], Xiao-Kui Guo [a], Xiao-Nong Zhou [a,b,**], Kokouvi Kassegne [a,*]

[a] *School of Global Health, Chinese Centre for Tropical Diseases Research, Shanghai Jiao Tong University School of Medicine, Shanghai 200025, China*

[b] *National Institute of Parasitic Diseases at Chinese Centre for Disease Control and Prevention (Chinese Centre for Tropical Diseases Research), National Health Commission of the People's Republic of China (NHC) Key Laboratory of Parasite and Vector Biology, World Health Organization (WHO) Collaborating Centre for Tropical Diseases, National Centre for International Research on Tropical Diseases of the Chinese Ministry of Science and Technology, Shanghai 200025, China*

ARTICLE INFO

Keywords:
Ticks
Haemaphysalis
MaxEnt model
Habitat suitability
Transmission risk
Environmental and bioclimatic factors
Chongming Island

ABSTRACT

Haemaphysalis ticks are pathogenic vectors that threaten human and animal health and were identified in Chongming, the third largest island in China. To understand the distribution of these ticks and determine their potential invasion risk, this study aimed to identify the habitat suitability of the dominant tick *H. flava* based on natural environmental factors. Geographic information system (GIS) images were combined with sample points from tick investigations to map the spatial distribution of *H. flava*. Data on 19 bioclimatic variables, environmental variables, and satellite-based landscapes of Chongming Island were retrieved to create a landcover map related to natural environmental determinants of *H. flava*. These data included 38 sites associated with the vectors to construct species distribution models with MaxEnt, a model based on the maximum entropy principle, and to predict habitat suitability for *H. flava* on Chongming Island in 2050 and 2070 under different climate scenarios. The model performed well in predicting the *H. flava* distribution, with a training area under the curve of 0.84 and a test area under the curve of 0.73. A habitat suitability map of the whole study area was created for *H. flava*. The resulting map and natural environment analysis highlighted the importance of the normalized difference vegetation index and precipitation in the driest month for the bioecology of *H. flava*, with 141.61 km^2 (11.77%), 282.94 km^2 (23.35%), and 405.30 km^2 (33.69%) of highly, moderately, and poorly suitable habitats, respectively. The distribution decreased by 135.55 km^2 and 138.82 km^2 in 2050 and 2070, respectively, under the shared socioeconomic pathway (SSP) 1.2.6 climate change scenario. However, under SSP 5.8.5, the total area will decrease by 128.5 km^2 in 2050 and increase by 151.64 km^2 in 2070. From a One Health perspective, this study provides good knowledge that will guide tick control efforts to prevent the spread of *Haemaphysalis* ticks or transmission risk of *Haemaphysalis*-borne infections at the human-animal-environment interface on the island.

1. Introduction

Ticks are specialized blood-sucking ectoparasites that attack vertebrates and transmit a variety of pathogens. They are important vectors of pathogens in domestic and wild animals and humans [1,2]. The epidemiological and epizootic significance of ticks is second only to that of mosquitoes [3].

In China, nine genera and 124 species of ticks have been reported [4]. Ticks have been identified in 10 of Shanghai's 17 districts [5], including Chongming [2]. Chongming Island, one of Shanghai's most

* Corresponding author. School of Global Health, Chinese Centre for Tropical Diseases Research, Shanghai Jiao Tong University School of Medicine, Shanghai 200025, China.

** Corresponding author. School of Global Health, Chinese Centre for Tropical Diseases Research, Shanghai Jiao Tong University School of Medicine, Shanghai 200025, China.

E-mail addresses: xiao-nong.zhou@sjtu.edu.cn (X.-N. Zhou), ephremk@hotmail.fr (K. Kassegne).

[1] Current address: Zhejiang University–University of Edinburgh International Institute, Zhejiang University, Haining, Zhejiang, 314400, China.

https://doi.org/10.1016/j.soh.2024.100068
Received 2 January 2024; Accepted 8 April 2024
Available online 16 April 2024

rural districts, accounts for 1/5 of the total area of Shanghai and is an irreplaceable strategic development space and ecological barrier of Shanghai [6]. The island is rich in forest vegetation and animal husbandry resources, providing conditions for the development of ticks, i.e., from eggs, larval ticks, and nymphal ticks to adult ticks [7]. Moreover, the Chongming Dongtan Bird National Nature Reserve is a home for migratory birds and provides shelter for wildlife; these animals are intermediate hosts of ticks, putting the island at risk of tick and tick-borne pathogen spread [8].

The transmission of tick-borne diseases relies on the presence of their vectors. A good understanding of their habitat distribution could provide insight into the potential risk of tick-borne disease transmission to susceptible hosts. Predictive geographical modelling based on the dependence of species distributions on environmental factors has been viewed as an important means to assess the impact of natural and anthropogenic environmental changes on organisms [9]. Environmental conditions play an important role in the life history of ticks [10,11], and climate influences the species distribution range, physiological responses, and survival in different regions [12,13]. Studies have predicted tick distributions in many parts of the world to assess the impact of bioclimatic factors on ticks, tick-borne diseases, and changes in distribution ranges [14–16].

Geographic information system (GIS) and remote sensing methods have been widely used in the field of wildlife and habitat suitability modelling. Species distribution models (SDMs) are empirical methods that quantify the realized environmental niches of species [17,18] and can be projected onto geographic space to predict potential distributions by relating species distribution data to a set of environmental variables [19]. Over the last few decades, SDMs have been developed rapidly, and a number of methods have emerged, including multilayer perceptron neural network (MLP-NN) [20], *Mahalanobis* typicality [21], and multiple-criteria evaluation [22], which have often been coupled with GIS to analyse species distributions [23]. Digital elevation models (DEMs), digital bioclimatic data from areas, and point location records are used as input data in machine learning methods or algorithms to map and analyse the current and future distributions of species [24,25]. Among the popular algorithms being used in modelling species distributions, the maximum entropy (MaxEnt) approach has gained significant advantage because it uses categorical and presence data only as input variables and can be applied to regions where data are scarce [26,27]. Models produced using MaxEnt can be easily understood and interpreted by providing valuable insights into the distribution and habitat suitability of a species [28], including under future conditions possibly impacted by climate change [29,30].

In a previous study, we found that *Haemaplysalis flava* is the dominant species of tick on Chongming Island [31]. *H. flava* is of primary importance to public health, medical and veterinary health, because it can cause lesions, dermatitis, blood loss, weight loss, and even death as a result of direct bites. It is also a vector of several pathogens, such as *Borrelia burgdorferi* [32,33], severe fever with thrombocytopenia syndrome virus, and tick-borne encephalitis virus [34]. To understand the ecological niches of ticks on the island, the present study aimed to provide a map of the habitat suitability of the dominant tick *H. flava* based on natural environmental factors. Starting from the sample points of our very recent tick investigation on the island, geographic location information on *H. flava* was combined with GIS images to map the spatial distribution of the ticks. In addition, we downloaded climate data from WorldClim and remote sensing data from Landsat-8 and Sentinel-2 from the Copernicus Open Access Hub and used the MaxEnt principle to construct species distribution models and to predict habitat suitability for *H. flava* on the island. We also evaluated the dominant variables restricting the geographical distribution of *H. flava* and the changes in habitat suitability areas under different future climate scenarios.

2. Materials and methods

2.1. Study area and survey data points

The study covered Chongming Island, where we recently surveyed for the presence of ticks and found *H. flava* dominant across the 18 towns of the island [2].

Chongming is an alluvial island at the mouth of the Yangtze River in eastern China covering 1202 km^2 (489 sq mi), with an estimated population of approximately 637,900 in 2022. Together with the islands Changxing and Hengsha, Chongming is the northernmost area of the provincial-level municipality of Shanghai. The island has a subtropical monsoon climate; the average annual high temperature is approximately 19.9 °C, the average annual low temperature is approximately 12.5 °C, the average annual precipitation is approximately 1129 mm, and the average relative humidity is approximately 80% [31].

All the location data of 38 sample sites across the whole island, along with longitude and latitude, were generated (Table S1) and were entered in Excel (Microsoft) and subsequently converted into ".csv" format, which is compatible with MaxEnt.

2.2. Environmental and bioclimatic variables

Variables associated with the environment were generated from WorldClim (https://worldclim.org/). Bioclimatic variables that reflect habitat allocation following the ecological niche of the species resulted from the long-term recording of monthly rainfall and temperature values (n = 19) [35]. The bioclimatic data with 30-s spatial resolution were downloaded with the WGS84 coordinate system. Table S2 shows the list of predictor variables used for this study. The Hadley Centre Global Environmental Model version 2 (HadGEM2) dataset was downloaded from the WorldClim portal and used to estimate the impact of future climate change on habitat suitability. To test habitat suitability for *H. flava* in the 2050s (2041–2060) and 2070s (2061–2080), future climate data were also downloaded from WorldClim based on the Beijing Climate Center-Climate System Model-Medium Resolution (BCC-CSM2-MR) climate system model, which includes three shared socioeconomic pathways (SSPs), i.e., the SSP5-8.5, SSP2-4.5, and SSP1-2.6 emission scenarios [36,37].

A CartoSat DEM (12.5 m resolution) [38] was used to extract topographic data. The DEM data that were obtained were mosaicked and resampled to a 10 m resolution, and the island-wide DEM data were subsequently cropped with administrative division vector files. Sentinel-2 was selected for imaging data from the European Space Agency (ESA) (https://scihub.copernicus.eu/). The images acquired were level-1C products, i.e., products that have been radiometrically and geometrically corrected and need to be atmospherically corrected using the Sen2cor module provided by the ESA. A level-2A product was obtained after atmospheric correction. Thereafter, the data were uniformly resampled to a resolution of 10 m, and the image was cropped using the Chongming administrative division boundary vector file to obtain each phase of the island's counties.

The boundary conditions were limited to the spatial extent of the Chongming area with a 100-m buffer [39]. To minimize multicollinearity and model overfitting and exclude extremely correlated variables, the Pearson multicollinearity test was performed with the SPSS statistical program, and variables with a correlation coefficient ≥0.85 were excluded [39,40].

The selection procedure for all variables was divided into two steps. First, all the variables (n = 27) were imported into the MaxEnt model, and those with a contribution rate of 0 were excluded. Second, all variables with a percent contribution rate greater than 0 were selected for Pearson correlation analysis. The smaller contribution rate of paired variables with a correlation coefficient ≥0.85 was excluded to finally obtain the variables for MaxEnt.

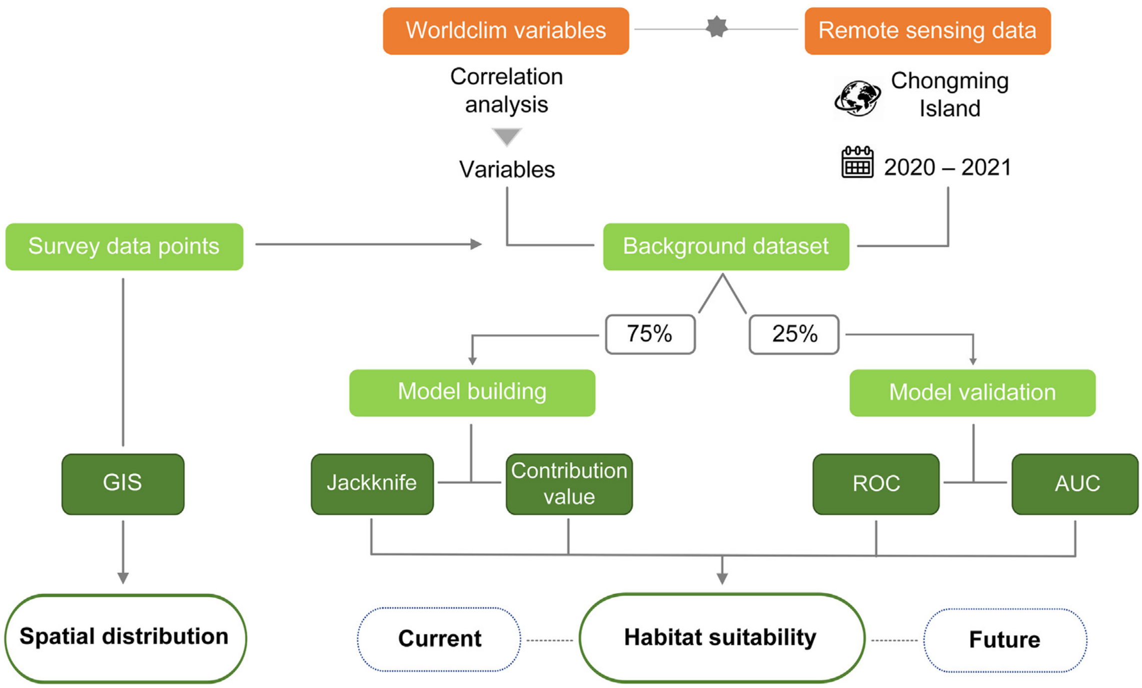

Fig. 1. The pipeline of the MaxEnt model workflow. The left side shows the process for mapping the survey data points; the right side shows the input factors, production of the model, and validation of habitat suitability. GIS: geographic information system; ROC: receiver operating curve; AUC: area under the curve.

2.3. MaxEnt distribution modelling and assessment

This study used the niche principal model of MaxEnt [41]. The method assumes that under certain known conditions, the system with the highest entropy is close to its true state. The distribution probability of the model was acquired under constraint conditions, and the habitat distributions of different spaces and times were predicted accordingly [42].

The habitat suitability of *H. flava* was predicted using MaxEnt 3.4.1. For modelling, 75% of the sample data were randomly selected in the training set, whereas 25% of the data were used in the testing set via bootstrap sampling, 10 replicates, and 500 maximum iterations [43,44].

We used the Jackknife test to investigate the importance of each variable for MaxEnt predictions and used the receiver operating curve (ROC) to assess the accuracy of the model [45]. The Jackknife test reflects the amount of gain obtained from all the variables in combination or from each variable in isolation. A variable with greater gain indicates that more contribution or information is contained in that variable towards species habitat distributions [39]. The model was evaluated by computing the area under the curve (AUC) value and average omission and prediction statistics [46]. The performance of the forecast model positively correlates with the area under the curve [47]. In general, the AUC lies between 0.5 and 1, and the evaluation criteria are as follows: AUC >0.9 is very good; 0.8 < AUC <0.9 is good; 0.7 < AUC <0.8 is acceptable; 0.6 < AUC <0.7 is bad; and AUC <0.6 is invalid [42]. Fig. 1 shows the pipeline of the MaxEnt model workflow used in this study.

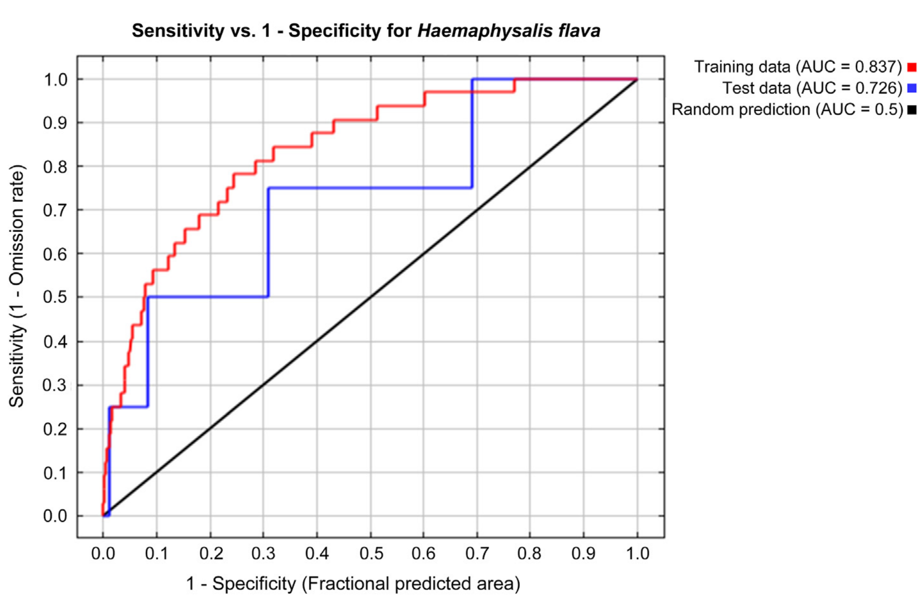

Fig. 2. Receiver operating curve (ROC) and the area under the curve (AUC) values of the MaxEnt model. The red curve indicates training data, the blue curve indicates test data, and the black line indicates random predictions.

2.4. Model application for prediction

According to two different projected bioclimatic change scenarios, geographical distribution maps for 2050 and 2070 were generated and compared with the current potential spatial distribution map.

In this study, a maximum value of 10 repetitions was selected as the prediction result and divided into suitable grades. ArcGIS 10.4 was used to convert the ".asc" file output by MaxEnt into a raster format file. Following the probability (P) of the presence of *H. flava*, the Intergovernmental Panel on Climate Change (IPCC) suitability grades were divided into four categories and are indicated by different colours, i.e., highly suitable habitat ($P \geq 0.53$, red), moderately suitable habitat ($0.34 \leq P < 0.53$, orange), poorly suitable habitat ($0.18 \leq P < 0.34$, cyan), and unsuitable habitat ($P < 0.18$, green). The modelling results of MaxEnt were imported into ArcGIS 10.4 and superimposed on the island vector map to obtain a distribution map of habitat suitability areas for *H. flava*. The SDMTools tool in ArcGIS was used to calculate the potential distribution areas.

3. Results

3.1. Spatial distribution and model performance

The spatial distribution of *H. flava* was mapped by combining the geographic location information of the 38 sample points with GIS images (Figure S1).

The training AUC value of the distribution model for *H. flava* was 0.837, and the test AUC value was 0.726, indicating that the performance of the model used in this study was "good" (Fig. 2, Figure S2).

3.2. Variable selection and variable contributions

The results of Pearson correlation matrix analysis performed to eliminate multicollinearity between the variables and improve the model performance are shown in Table 1.

The cumulative percentage contribution and permutation importance of individual variables were also computed. The Jackknife test built in MaxEnt generated a bioclimate-based distribution model for *H. flava*. The test results revealed that the normalized difference vegetation index (NDVI), precipitation of the driest month (bio14), elevation, precipitation of the coldest quarter (bio19), normalized difference bare soil index (NDBSI), precipitation of the warmest quarter (bio18), isothermality (bio3), precipitation of the driest quarter (bio17), and slope were the variables that were most sensitive to the models. By comparing the regularized training gains with each single variable (Fig. 3A), we found that the regularized training gains of the NDVI, bio14, elevation, and bio19 were important for determining the habitat suitability of *H. flava*. The NDVI (33.4%) was the most important variable that contributed to the models, while bio14, elevation, and bio19 contributed 23.0%, 11.6% and 11.5%, respectively (Table 2). The response curve obtained by using only a single environmental variable clarified the relationship between key environmental variables and the probability of *H. flava* presence (Fig. 3B, Figures S3-S8). The results showed that the highest suitable ranges of NDVI, bio14, elevation, and bio19 were 0.7–0.8, 32–34 mm, 6–8 m, and 116–122 mm, respectively (Fig. 3B).

3.3. Areas suitable for H. flava habitat

The habitat suitability of *H. flava* on Chongming Island under current bioclimatic conditions was mapped (Fig. 4A, Figure S9). The results showed that the highly suitable habitats (141.61 km^2) were located mainly in the southeastern part of the island, near the urban area of Shanghai. This result is consistent with the occurrence points on the island where the ticks were collected (Figure S1, Figure S9). In particular, large natural ecological areas, e.g., Dongping National Forest Park, the

Table 1
Pearson correlation analysis of natural environmental variables ($r < 0.85$).

Layer	NDVI	NDBSI	Humidity	Aspect	Slope	Altitude	Bio1	Bio3	Bio4	Bio6	Bio7	Bio9	Bio11	Bio13	Bio14	Bio15	Bio17	Bio18	Bio19	Road	River
NDVI	1																				
NDBSI	−0.8016	1																			
Humidity	−0.5781	0.9178	1																		
Aspect	0.2536	−0.3144	−0.2805	1																	
Slope	0.2578	−0.3174	−0.2793	0.4800	1																
Altitude	0.3845	−0.5010	−0.4629	0.2959	0.3448	1															
Bio1	−0.0599	0.0557	0.0647	0.0192	0.0453	0.0892	1														
Bio3	0.1002	−0.0779	−0.0720	0.0231	0.0227	0.0002	−0.6279	1													
Bio4	0.0791	−0.0689	−0.0719	−0.0126	−0.0430	−0.0792	−0.8989	0.5220	1												
Bio6	−0.0781	0.0664	0.0704	0.0079	0.0316	0.0675	0.9596	−0.7500	−0.9062	1											
Bio7	0.0966	−0.0780	−0.0783	−0.0001	−0.0236	−0.0482	−0.8979	0.7602	0.9329	−0.9715	1										
Bio9	−0.0226	0.0342	0.0490	0.0150	0.0304	0.0839	0.6935	−0.4735	−0.6437	0.6694	−0.6365	1									
Bio11	−0.0697	0.0629	0.0694	0.0164	0.0461	0.0880	0.9821	−0.6089	−0.9603	0.9699	−0.9416	0.6918	1								
Bio13	0.0823	−0.0567	−0.0560	−0.0017	−0.0275	−0.0124	−0.7302	0.4427	0.8525	−0.7511	0.8049	−0.4393	−0.7924	1							
Bio14	−0.0713	0.0523	0.0436	−0.0146	−0.0175	0.0451	0.4359	−0.6226	−0.3511	0.4914	−0.4682	0.4174	0.4073	−0.1657	1						
Bio15	0.0859	−0.0659	−0.0704	−0.0080	−0.0356	−0.0351	−0.8435	0.5583	0.8920	−0.8491	0.8719	−0.5688	−0.8773	0.9246	−0.3696	1					
Bio17	−0.0111	0.0163	0.0141	−0.0175	−0.0176	−0.0153	−0.1893	−0.1148	0.3942	−0.1991	0.2581	−0.0569	−0.2710	0.5364	0.3797	0.2886	1				
Bio18	0.0741	−0.0571	−0.0566	−0.0061	−0.0311	−0.0367	−0.8319	0.5340	0.9168	−0.8572	0.8790	−0.5810	−0.8832	0.8999	−0.3417	0.9199	0.4647	1			
Bio19	−0.0589	0.0468	0.0459	−0.0088	−0.0026	0.0368	0.5693	−0.7934	−0.3088	0.6296	−0.5394	0.4593	0.4949	−0.1753	0.7046	−0.4073	0.4664	−0.3288	1		
Road	−0.9269	0.2704	−0.0030	0.0050	−0.1674	−0.1217	−0.5935	−0.5483	−0.0522	0.2519	0.5033	−0.4879	−0.4201	0.6252	0.2520	0.5532	−0.6152	−0.4002	0.0000	1	
River	−0.2016	0.8574	−0.7307	−0.0017	−0.1968	−0.0235	−0.3185	−0.3397	0.2017	0.4731	0.2065	−0.3095	−0.5301	0.5242	0.4301	0.0629	−0.2984	−0.1145	0.0000	0.1371	1

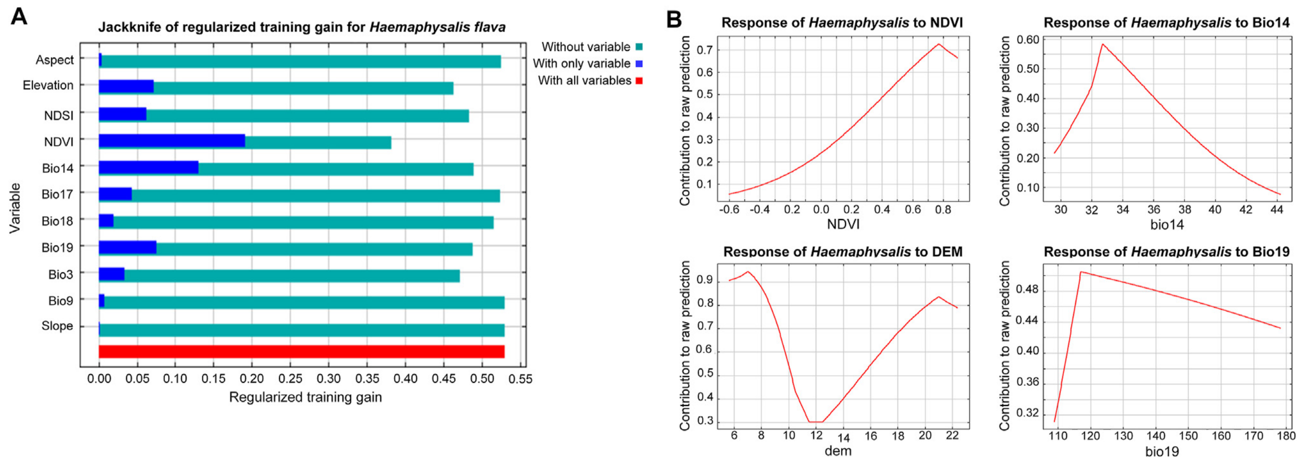

Fig. 3. Contribution of natural environmental variables to *H. flava* distribution on Chongming Island. (A) Contribution of natural environmental variables to the models according to Jackknife analysis. The Jackknife test for variable importance in the models is shown. The variable with the highest gain when used in isolation was the NDVI, which therefore appears to have the most useful information. The values shown are averages over replicate runs. **(B)** Response curves of *H. flava* habitat suitability to the NDVI, precipitation of the driest month, altitude, and precipitation of the coldest quarter. NDVI, normalized difference vegetation index; Bio14, precipitation of the driest month; DEM, digital elevation model; Bio19, precipitation of the coldest quarter.

Xisha Wetland, the Mingzhu Lake Scenic Area, and the Dongtan Bird National Nature Reserve, are found in highly suitable habitats. The moderately suitable habitats (282.94 km^2) were mainly distributed around high-risk areas. Poorly suitable habitats (405.3 km^2) and unsuitable habitats (373.13 km^2) were located in the northern part of the island, near the town of Gangyan in the middle of Chongming Island, and in the southeastern part of Changxing Island. The unsuitable habitats also include the coastal areas of Chongming (main) Island, Hengsha Island, and Changxing Island.

The overall trends of the predicted habitat suitability areas for *H. flava* under the future bioclimatic scenarios (SSP1-2.6, SSP2-4.5, and SSP5-8.5) are shown in Fig. 4**B** and 5. Areas of highly, moderately, and poorly suitable habitats showed a significant increasing trend (Table S3).

By the 2050s, the unsuitable habitat area will increase to 478.02 km^2 (SSP1-2.6), 456.58 km^2 (SSP2-4.5), and 465.99 km^2 (SSP5-8.5), while the poorly suitable habitat area will decrease to 355.85 km^2 (SSP1-2.6), 351.62 km^2 (SSP2-4.5), and 359.19 km^2 (SSP5-8.5). In addition, the area of moderately suitable habitat will decrease to 233.58 km^2 (SSP1-2.6), 255.56 km^2 (SSP2-4.5), and 249.28 km^2 (SSP5-8.5), while the area of highly suitable habitat will decrease to 135.54 km^2 (SSP1-2.6), 139.22 km^2 (SSP2-4.5), and 128.51 km^2 (SSP5-8.5) (Fig. 4B). By the 2070s, the highly suitable habitat areas are projected to increase to 138.82 km^2 (SSP1-2.6), 141.97 km^2 (SSP1-2.6), and 151.64 km^2 (SSP5-8.5), and the moderately suitable habitats are expected to increase to 254.45 km^2 (SSP1-2.6), 264.17 km^2 (SSP2-4.5), and 298.30 km^2 (SSP5-8.5), while the poorly suitable habitat areas are expected to increase to 346.43 km^2 (SSP1-2.6), 364.56 km^2 (SSP2-4.5), and 388.15 km^2 (SSP5-8.5) (Fig. 4B).

Table 2
Percent contribution of selected variables for the model.

Variable	Percentage contribution (%)
NDVI	33.4
Bio14	23.0
Elevation	11.6
Bio19	11.5
NDBSI	7.1
Bio18	5.7
Bio3	3.9
Bio17	2.6
Slope	1.3
Aspect	0
Bio9	0

Under the SSP1-2.6 scenario, the habitat suitability of *H. flava* on the island would account for 30.68% (2050s) and 33.02% (2070s) of the total suitable habitat area, including moderately suitable and highly suitable areas, respectively. Under SSP2-4.5, 30.68% (2050s) and 33.76% (2070s) of the total suitable habitat would occur, while 31.40% (2050s) and 37.40% (2070s) of the total suitable habitat would occur under the SSP5-8.5 future climate scenario.

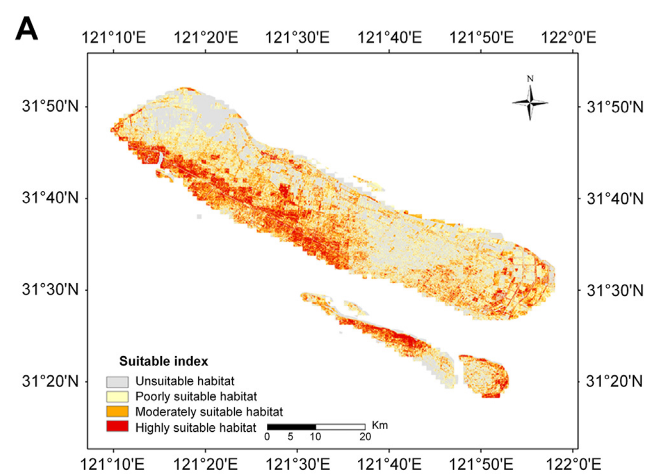

B

Period	Prediction areas (km^2)				
	Unsuitable	Poor	Moderate	High	Total
Current	373.13	405.30	282.94	141.61	1202.98
2050 (SSP 126)	478.02	355.85	233.58	135.55	1202.98
2070 (SSP 126)	463.29	346.43	254.45	138.82	1202.98
2050 (SSP 245)	456.58	351.62	255.56	139.22	1202.98
2070 (SSP 245)	432.29	364.56	264.17	141.97	1202.98
2050 (SSP 585)	465.99	359.19	249.28	128.51	1202.98
2070 (SSP 585)	364.89	388.15	298.30	151.64	1202.98

Unsuitable, unsuitable habitat; Poor, poorly suitable habitat; Moderate, moderately suitable habitat; High, highly suitable habitat

Fig. 4. Habitat suitability of response to the NDVI for *H. flava* on Chongming Island. (A) Habitat suitability map of response to the NDVI for *H. flava* under current bioclimatic conditions. NDVI, normalized difference vegetation index. **(B)** Distribution of habitat suitability areas for *H. flava* over time.

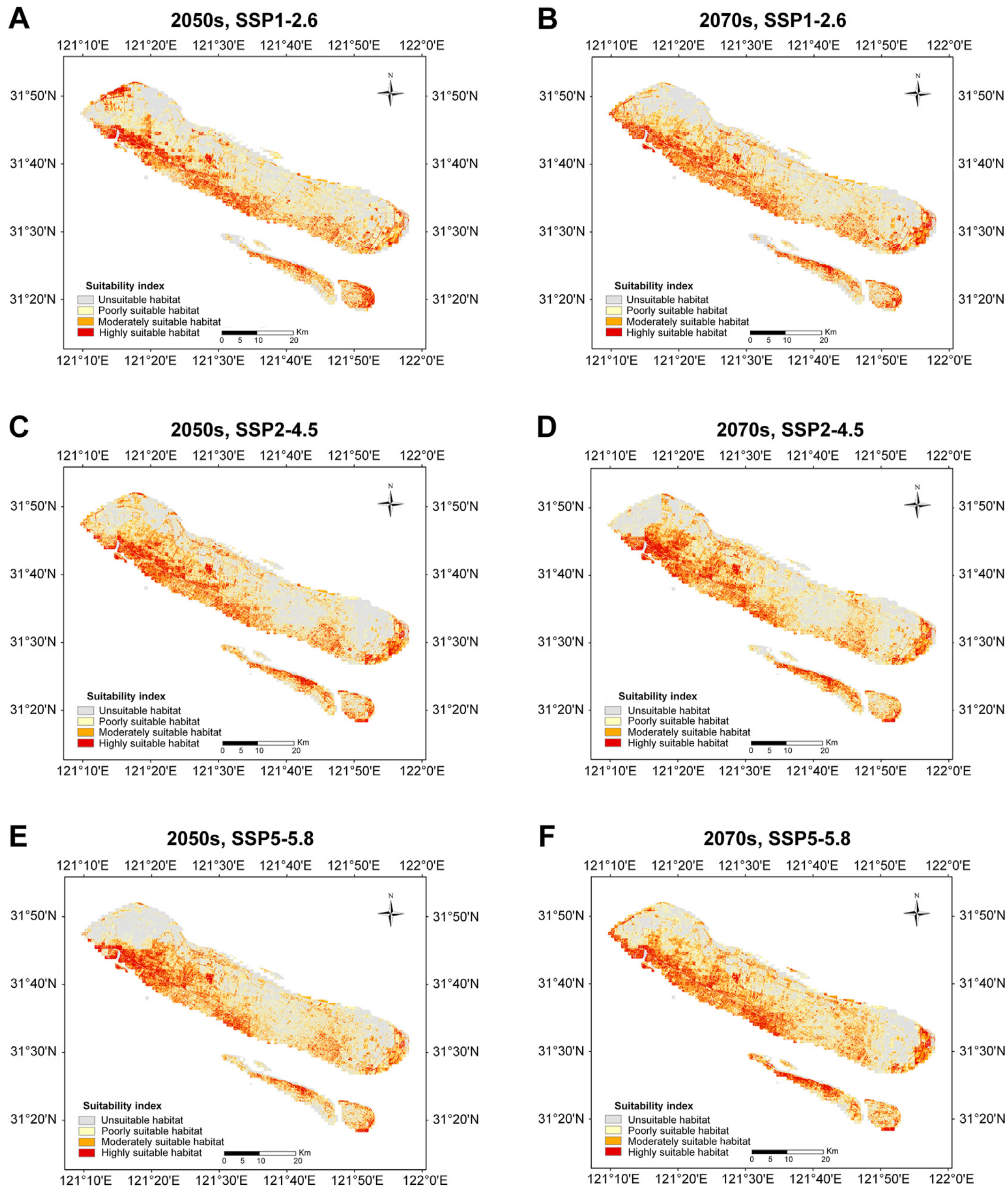

Fig. 5. Map of habitat suitability areas for *H. flava* under future bioclimatic scenarios on Chongming Island. SSP1-2.6 represents a sustainable development scenario with low greenhouse gas emission levels. SSP2-4.5 indicates that greenhouse gas emissions are at a medium level; that is, the future socioeconomic development model will continue to develop on the basis of the current model. SSP5-8.5 is a scenario based on full socioeconomic development and represents a high level of greenhouse gas emissions [33].

4. Discussion

Recently, the growing awareness of emerging tick-borne pathogens has greatly inspired investigations on ticks and tick-borne diseases in China. In this study, the spatial distribution of habitat suitability for *H. flava* was mapped, and the MaxEnt model was applied to simulate the distribution based on natural environmental factors.

Nineteen of the 38 sampling points were distributed in the highly suitable habitat area, 10 and five were distributed in the moderately and poorly suitable habitat areas, respectively, and four distribution points were found in the unsuitable habitat area, showing that the predicted results were credible. The NDVI is the most widely used vegetation index and can, to a certain extent, eliminate the effects of radiation errors caused by various factors and better reflect vegetation cover and growth [48]. The response curves obtained from this study showed that the presence of *H. flava* ticks was most likely when the NDVI reached 0.7–0.8.

As comprehensive natural environmental factors, elevation, temperature, moisture, and light all vary with elevation and have effects on the physiological function and reproduction of animals [49,50]. The effect of elevation on the geographic distribution of ticks may not be solely due to temperature. A previous study showed that ticks and tick-borne diseases can gradually spread to high altitudes with global warming [51]. Ticks have distinct limits of tolerance to elevation, so elevation is also a major natural environmental factor affecting tick habitat suitability. Among the bioclimatic factors assessed in this study, the precipitation of the driest month and the precipitation of the coldest quarter strongly contributed to the models of habitat suitability for *H. flava*.

Studies suggest that dryness may be a limiting factor for the activity of ticks [52]. When the humidity in the air is too low, the risk of desiccation and dehydration during the host-seeking process increases. Adequate relative humidity not only increases the survival rate of ticks at all life stages but also decreases the risk of drying out and dehydration during host searching [53]. The greater the humidity is, the greater the survival rate of ticks at all life stages. Winter precipitation results in the formation of a snow layer with moisture retention that is ideal for tick survival during the season [54]. Most areas of the country have precipitation that meets suitable conditions for the development of ticks [55]. Additionally, next to water retention, e.g., lakes, humidity is also greater than that elsewhere, and the presence of ticks is more likely in places close to forest lakes. Furthermore, Heath [56] showed that ticks were distributed from a critical temperature of 9–12 °C to a lethal temperature close to 40 °C. This evidence is consistent with the findings obtained from the present study.

The environmental factors affecting the geographical distribution of species include climate, topography, vegetation, soil, land use type, and human disturbance. At small habitat scales, vegetation, interspecific competition and human disturbance are the most important factors influencing animal habitat selection, while at large spatial scales, geographical distribution is mainly governed by climatic factors. This study focused on the geographic distribution trends of *H. flava*. Bioclimatic changes influence the distribution patterns of ticks. Factors such as host distribution, human-environment modifications, and livestock that may affect tick distribution [57,58] were not included in the study because of a lack of available data under future scenarios. To improve the transferability of the established model, the present study applied the MaxEnt model to future climate variables and accurately predicted potentially suitable habitat areas for *H. flava*. A similar previous study also reported the accuracy of climate-based forecasts of pathogen spread [59].

The three shared socioeconomic pathway (SSP) scenarios, SSP1-2.6, SSP3-7.0, and SSP5-8.5, applied in this study represent different future bioclimates with increasing CO_2 emissions and rising global temperatures. The present study showed that the habitat suitability area for *H. flava* on Chongming Island decreased significantly with increasing carbon emissions under all three future bioclimatic scenarios, especially in the moderately suitable zone. Although ticks are highly adaptable to changes in environmental temperature, the increasing frequency and intensity of extreme climatic events and either too high or too low temperatures could negatively affect the survival of hard ticks across ditches, which could lead to a reduction in the distribution of future fitness zones [60]. Under the SSP5-8.5 climate scenario of severe global warming, the distribution range will continue to expand. However, with the development of ecological civilization, under the continuous promotion of global biodiversity conservation and under the guidance of the integrated management concept of “mountain, water, forest, lake, grass, sand, and ice” and the “double carbon” strategy, the future climate under the SSP5-8.5 scenario would be very unlikely to occur. Therefore, habitat suitability areas for *H. flava* may continue to decrease under such future climate change.

Habitat suitability areas for *H. flava* on the island will generally decrease; however, moderately and highly suitable areas will become more widespread. This is expected around forests because the broad-leaved trees planted along both sides of roads and between fields provide adequate conditions for ticks to avoid exposure to direct sunlight [61]. Notably, the southwestern edge of the island, where many natural reserves are located, revealed a spotty distribution and habitat suitability pattern for *H. flava*. These natural reserves displayed moderate or high presence rates; nevertheless, there may be tick presence, given that they are located within the path of migratory birds [62]. Previous studies have reported that migratory birds play an important role in extending both plant and tick distributions [63]. However, studies on the impact of migratory birds and tick distributions in these areas are needed in the future for effective control of tick-borne infections via the One Health approach [64–67].

Given that this study was based on topographical and bioclimatic factors and used the MaxEnt principle, there is a future scope to explore other dimensions, such as distance from the road, distance from settlement zones, change in land use/land cover, and interspecies competition, which might impact habitat suitability using various other algorithms, such as multiple-criteria evaluation (MCE), the multiple-layer perceptron neural network (MLP-NN) approach, and the *Mahalanobis* typicality approach.

Although MaxEnt achieves the best model performance with the significant advantage of using categorical and presence data as input variables, other models with different input sets may yield greater predictions. Therefore, an example of a limitation of our study is that variables such as domestic animals, urban and peri-urban cultivated and paved areas, and wildlife that may impact tick densities [58,59] were not included. However, studies on the influence of vertebrate hosts during different life stages of *Haemaphysalis* ticks on their distribution and on the influence of habitat suitability of *Haemaphysalis* ticks on host distribution are needed.

5. Conclusion

Climate change and environmental variables impact the habitat suitability of *H. flava* on Chongming Island. The NDVI strongly contributed to the distribution and habitat suitability of *H. flava*. In addition, two variables, precipitation of the driest month (bio14), which is dependent on temperature, and precipitation in the coldest quarter (bio19), were found to be the most influential bioclimatic variables in the models. Overall, the potential distribution range of *H. flava* on the island will decrease under the premise of human protection. Additionally, high-suitability areas will not change significantly, and habitat suitability areas are expected to be limited to the central core zone of nature reserves. These findings indicate that the dissemination of *Haemaphysalis* ticks is unlikely to increase in the next 50 years. However, surveillance and early warnings should be strengthened to prevent the eventual spread of ticks or tick-borne pathogen transmission at the One Health interface.

Funding

This study was financially supported in part by The International Joint Laboratory on Tropical Diseases Control in the Greater Mekong Subregion fund (21,410,750,200) of the Science and Technology Commission of Shanghai, China and The Science and Technology Innovation Project fund of the School of Global Health, Shanghai Jiao Tong University School of Medicine (SGHKJCX2021-05, SGHKJCX2021-04), China. The sponsor played no role in the study design; in the collection, analysis, or interpretation of the data; in the writing of the report; or in the decision to submit the article for publication.

Author contributions

Conception and study design: KK and X-NZ. Survey data collection points: S-WF, H-QZ, J-XY, S-ZS, and KK. Data collection, analysis and modelling: S-WF, J-BX, and SX. Supervision: X-NZ and KK. Writing-original draft: S-WF. Revision and editing: SL, XY-F, X-KG, X-NZ, and KK. All the authors contributed to the article and approved the submitted version.

Data availability statement

The data are not publicly available because they need to be used in future work. However, any requirement of data should be addressed to the corresponding author (ephremk@hotmail.fr) upon reasonable request.

Declaration of competing interest

Xiao-Nong Zhou is the Editor-in-Chief of *Science in One Health*, Xiao-Kui Guo is the Deputy Editor-in-Chief of this journal. They were not involved in the peer review or handling of the manuscript. The authors have no other competing interests to disclose.

Acknowledgements

The authors thank Dr. Shang Xia [National Institute of Parasitic Diseases at the Chinese Centre for Disease Control and Prevention (Chinese Centre for Tropical Diseases Research] for the constructive comments during the development of the models.

Abbreviations

GIS	Geographic information system
SDMs	Species distribution models
MLP-NN	Multilayer perceptron neural network
DEMs	Digital elevation models
MaxEnt	Maximum entropy
HadGEM2	Hadley Centre Global Environmental Model version 2
BCC-CSM2-MR	Beijing Climate Center-Climate System Model-Medium Resolution
SSPs	Shared socioeconomic pathways
ESA	European Space Agency
ROC	Receiver operating curve
AUC	Area under the curve
IPCC	Intergovernmental Panel on Climate Change
NDVI	Normalized difference vegetation index
NDBSI	Normalized difference bare soil index
MCE	Multiple-criteria evaluation

Appendix A. Supplementary data

Supplementary data to this article can be found online at https://doi.org/10.1016/j.soh.2024.100068.

References

[1] J. de la Fuente, A. Estrada-Pena, J.M. Venzal, K.M. Kocan, D.E. Sonenshine, Overview: ticks as vectors of pathogens that cause disease in humans and animals, Front. Biosci. J. Vis. Literacy 13 (2008) 6938–6946.
[2] S. Fei, H. Zhao, J. Yin, L. Wang, Z. Sun, W. Zhang, Y. Zhang, K. Dong, S. Lyu, X. Guo, et al., Molecular identification and genetic characterization of public health threatening ticks - chongming island, China, 2021-2022, China CDC Wkly 5 (2023) 815–821.
[3] L.Q. Fang, K. Liu, X.L. Li, S. Liang, Y. Yang, H.W. Yao, R.X. Sun, Y. Sun, W.J. Chen, S.Q. Zuo, et al., Emerging tick-borne infections in mainland China: an increasing public health threat, Lancet Infect. Dis. 15 (2015) 1467–1479.
[4] G.P. Zhao, Y.X. Wang, Z.W. Fan, Y. Ji, M.J. Liu, W.H. Zhang, X.L. Li, S.X. Zhou, H. Li, S. Liang, et al., Mapping ticks and tick-borne pathogens in China, Nat. Commun. 12 (2021) 1075.
[5] Q. Liu, F.R. Wei, D. Zhu, Q.X. Lan, W.Q. Shi, Y. Zhang, Investigation of ticks parasitizing on bodies of dogs in Shanghai], Zhongguo Xue Xi Chong Bing Fang Zhi Za Zhi 24 (2012) 537–539, 543.
[6] B. Huang, Z. Ouyang, H. Zheng, H. Zhang, X. Wang, Construction of an eco-island: a case study of Chongming Island, China, Ocean Coast Manag. 51 (2008) 575–588.
[7] C.L. Wan, HQ: Chongming World-Class Ecological Island Construction Index System and Evaluation Research Northern Economy and Trade, vol. 7, 2021, pp. 134–136 (in Chinese).
[8] G. Hasle, Transport of ixodid ticks and tick-borne pathogens by migratory birds, Front. Cell. Infect. Microbiol. 3 (2013) 48.
[9] J. Hernández-Urcera, F.J. Murillo, M. Regueira, M. Cabanellas-Reboredo, M. Planas, Preferential habitats prediction in syngnathids using species distribution models, Mar. Environ. Res. 172 (2021) 105488.
[10] J.A. Wiens, D. Stralberg, D. Jongsomjit, C.A. Howell, M.A. Snyder, Niches, models, and climate change: assessing the assumptions and uncertainties, Proc. Natl. Acad. Sci. U. S. A. 106 (Suppl 2) (2009) 19729–19736.
[11] C. Magdaş, V.A. Magdaş, A.D. Mihalca, H. Baciu, C.M. Gherman, C.L. Ştefănuţ, M. Lefkaditis, V. Cozma, Laboratory development of Dermacentor marginatus ticks (Acari: ixodidae) at two temperatures, Exp. Appl. Acarol. 67 (2015) 309–315.
[12] L.Y. Acevedo-Gutiérrez, L.E. Paternina, A.F. Londoño, G. Parra-Henao, J.D. Rodas, Potential models of the geographic and climatic distribution of the Amblyomma cajennense complex (Acari: ixodidae), a potential vector of *Rickettsia rickettsii* in Colombia, Biomedica 38 (2018) 534–544.
[13] R.K. Raghavan, A.T. Peterson, M.E. Cobos, R. Ganta, D. Foley, Current and future distribution of the lone star tick, Amblyomma americanum (L.) (Acari: ixodidae) in north America, PLoS One 14 (2019) e0209082.
[14] T.P. Feria-Arroyo, I. Castro-Arellano, G. Gordillo-Perez, A.L. Cavazos, M. Vargas-Sandoval, A. Grover, J. Torres, R.F. Medina, A.A. de León, M.D. Esteve-Gassent, Implications of climate change on the distribution of the tick vector *Ixodes scapularis* and risk for Lyme disease in the Texas-Mexico transboundary region, Parasites Vectors 7 (2014) 199.
[15] J.R. Soucy, A.M. Slatculescu, C. Nyiraneza, N.H. Ogden, P.A. Leighton, J.T. Kerr, M.A. Kulkarni, High-resolution ecological niche modeling of *Ixodes scapularis* ticks based on passive surveillance data at the northern frontier of lyme disease emergence in north America, Vector Borne Zoonotic Dis. 18 (2018) 235–242.
[16] I. Rochlin, Modeling the asian longhorned tick (Acari: ixodidae) suitable habitat in north America, J. Med. Entomol. 56 (2019) 384–391.
[17] F. Raffini, G. Bertorelle, R. Biello, G. D'Urso, D. Russo, L. Bosso, From nucleotides to satellite imagery: approaches to identify and manage the invasive pathogen xylella fastidiosa and its insect vectors in europe, Sustainability 12 (2020) 4508.
[18] M.W.F. Howse, J. Haywood, P.J. Lester, Bioclimatic modelling identifies suitable habitat for the establishment of the invasive European paper wasp (hymenoptera: vespidae) across the southern hemisphere, Insects 11 (2020) 784.
[19] C.J. Ellis, R. Yahr, R. Belinchón, B.J. Coppins, Archaeobotanical evidence for climate as a driver of ecological community change across the anthropocene boundary, Global Change Biol. 20 (2014) 2211–2220.
[20] C. Capinha, E. Gomes, E. Reis, J. Rocha, C.A. Sousa, V.E. do Rosário, A.P. Almeida, Present habitat suitability for Anopheles atroparvus (Diptera, Culicidae) and its coincidence with former malaria areas in mainland Portugal, Geospat Health 3 (2009) 177–187.
[21] T.R. Etherington, Mahalanobis distances and ecological niche modelling: correcting a chi-squared probability error, PeerJ 7 (2019) e6678.
[22] R. Store, J. Jokimäki, A GIS-based multi-scale approach to habitat suitability modeling, Ecol. Model. 169 (2003) 1–15.
[23] W. Schröder, GIS, geostatistics, metadata banking, and tree-based models for data analysis and mapping in environmental monitoring and epidemiology, Int J Med Microbiol 296 (Suppl 40) (2006) 23–36.
[24] S.J. Phillips, Modeling of species distributions with Maxent: new extensions and a comprehensive evaluation, Ecography 31 (2008) 161–175, 2008 v.2031 no.2002.
[25] Y.-s. Wang, B.-y. Xie, F.-h. Wan, Q.-m. Xiao, L.-y. Dai, The potential geographic distribution of radopholus similis in China, Agric. Sci. China 6 (2007) 1444–1449.
[26] N.S. Morales, I.C. Fernández, V. Baca-González, MaxEnt's parameter configuration and small samples: are we paying attention to recommendations? A systematic review, PeerJ 5 (2017) e3093.
[27] J. Wan, G.-j. Qi, J. Ma, Y. Ren, R. Wang, S. McKirdy, Predicting the potential geographic distribution of Bactrocera bryoniae and Bactrocera neohumeralis (Diptera: tephritidae) in China using MaxEnt ecological niche modeling, J. Integr. Agric. 19 (2020) 2072–2082.
[28] X. Tang, Y. Yuan, X. Li, J. Zhang, Maximum entropy modeling to predict the impact of climate change on pine wilt disease in China, Front. Plant Sci. 12 (2021) 652500.
[29] Z. Zhang, S.-y. Xu, C. Capinha, R. Weterings, T. Gao, Using species distribution model to predict the impact of climate change on the potential distribution of Japanese whiting Sillago japonica, Ecol. Indicat. 104 (2019) 333–340.
[30] A.M. Gormley, D.M. Forsyth, P. Griffioen, M. Lindeman, D.S. Ramsey, M.P. Scroggie, L. Woodford, Using presence-only and presence-absence data to estimate the current and potential distributions of established invasive species, J. Appl. Ecol. 48 (2011) 25–34.
[31] China Meteorological Administration. Retrieved 26 August 2023. https://cma.gov.cn/en2014/.
[32] J. Cao, Q. Yang, J. Zhang, Y. Zhou, H. Zhang, H. Gong, J. Zhou, Seroprevalence survey of Babesia gibsoni infection and tick species in dogs in East China, Vet. Parasitol. 214 (1–2) (2015) 12–15.
[33] Y.Z. Zhang, J. Xu, The emergence and cross species transmission of newly discovered tick-borne Bunyavirus in China, Curr Opin Virol 16 (2016) 126–131.
[34] T. Allen, K.A. Murray, C. Zambrana-Torrelio, S.S. Morse, C. Rondinini, M. Di Marco, P. Daszak, Global hotspots and correlates of emerging zoonotic diseases, Nat. Commun. 8 (1) (2017) 1124.
[35] W.G. Alemu, M.C. Wimberly, Evaluation of remotely sensed and interpolated environmental datasets for vector-borne disease monitoring using in situ observations over the amhara region, Ethiopia, Sensors 20 (2020) 1316.
[36] S.E.H.R. Fick, WorldClim 2: new 1 km spatial resolution climate surfaces for global land areas, Int. J. Climatol. 37 (2017) 4302–4315.
[37] R. Maruthadurai, B. Das, R. Ramesh, Predicting the invasion risk of rugose spiraling whitefly, Aleurodicus rugioperculatus, in India based on CMIP6 projections by MaxEnt, Pest Manag. Sci. 79 (2023) 295–305.
[38] L.S. Tang Xinming, Li Tao, Gao Yandong, Shubi Zhang, Qianfu Chen, Review on global digital e;evation products, National Remote Sensing Bulletin (2021) 167–181.
[39] X. Dai, W. Wu, L. Ji, S. Tian, B. Yang, B. Guan, D. Wu, MaxEnt model-based prediction of potential distributions of Parnassiawightiana (Celastraceae) in China, Biodivers. Data J. 10 (2022) e81073.
[40] M. Li, J. He, Z. Zhao, R. Lyu, M. Yao, J. Cheng, L. Xie, Predictive modelling of the distribution of Clematis sect. Fruticella s. str. under climate change reveals a range expansion during the Last Glacial Maximum, PeerJ 8 (2020) e8729.
[41] J. Elith, S.J. Phillips, T.J. Hastie, M. Dudík, Y.E. Chee, C.J. Yates, A statistical explanation of MaxEnt for ecologists, Divers, Distrib 17 (2011) 43–57.
[42] S.J. Phillips, R.P. Anderson, R.E. Schapire, Maximum entropy modeling of species geographic distributions, Ecol. Model. 190 (2006) 231–259.
[43] Y. Zhang, J. Tang, G. Ren, K. Zhao, X. Wang, Global potential distribution prediction of Xanthium italicum based on Maxent model, Sci. Rep. 11 (2021) 16545.
[44] M. Yang, H. Zhao, X. Xian, H. Liu, J. Li, L. Chen, W. Liu, Potential global geographical distribution of Lolium temulentum L. under climate change, Front. Plant Sci. 13 (2022) 1024635.

[45] M.T. Robinson, A.A. Hoffmann, The pest status and distribution of three cryptic blue oat mite species (Penthaleus spp.) and redlegged earth mite (Halotydeus destructor) in southeastern Australia, Exp. Appl. Acarol. 25 (2001) 699–716.
[46] A.S.J.v. Proosdij, M.S.M. Sosef, J.J. Wieringa, N. Raes, Minimum required number of specimen records to develop accurate species distribution models, Ecography 39 (2016) 542–552.
[47] J.H. Elith, C. Graham, R.P. Anderson, M. Dudík, S. Ferrier, A. Guisan, R.J. Hijmans, F. Huettmann, J.R. Leathwick, A. Lehmann, et al., Novel methods improve prediction of species' distributions from occurrence data, Ecography 29 (2006) 129–151.
[48] C.J. Tucker, Red and photographic infrared linear combinations for monitoring vegetation, Rem. Sens. Environ. 8 (1979) 127–150.
[49] M. Li, X. Gao, S. Yang, Z. Duan, W. Cao, H. Liu, Effects of environmental factors on natural reproduction of the four major Chinese carps in the Yangtze River, China, Zool. Sci. (Tokyo) 30 (2013) 296–303.
[50] J.Y. Kim, C. Seo, S. Hong, S. Lee, S.H. Eo, Altitudinal range-size distribution of breeding birds and environmental factors for the determination of species richness: an empirical test of altitudinal Rapoport's rule and non-directional rescue effect on a local scale, PLoS One 14 (2019) e0203511.
[51] L. Gilbert, Altitudinal patterns of tick and host abundance: a potential role for climate change in regulating tick-borne diseases? Oecologia 162 (2010) 217–225.
[52] Z.Y. Zhang Chenchen, Research progress on biological characteristics of common tick species and tick- borne diseases in China, Int. J. Mod. Phys. 42 (3) (2015) 184–188.
[53] Z.Z. Liu Xufei, Wei Wang, Jianxu Zheng, Wei Wanhong, Li Kai, Influence of weather factors on questing activity of haemaphysails longicornis, Sci. Silvae Sin. 56 (6) (2018) 68–75.
[54] M. Walter, K. Brugger, F. Rubel, The ecological niche of Dermacentor marginatus in Germany, Parasitol. Res. 115 (2016) 2165–2174.
[55] E.I. Korenberg, Chapter 4. Recent epidemiology of tick-borne encephalitis an effect of climate change? Adv. Virus Res. 74 (2009) 123–144.
[56] A. Heath, Biology, ecology and distribution of the tick, Haemaphysalis longicornis Neumann (Acari: ixodidae) in New Zealand, N. Z. Vet. J. 64 (2016) 10–20.
[57] J. Sunday, A. Bates, N. Dulvy, Thermal tolerance and the global redistribution of animals, Nat. Clim. Change 2 (2012) 686–690.
[58] A. Estrada-Peña, N. Alexander, G.R. Wint, Perspectives on modelling the distribution of ticks for large areas: so far so good? Parasites Vectors 9 (2016) 179.
[59] A.M. Schatz, A.M. Kramer, J.M. Drake, Accuracy of climate-based forecasts of pathogen spread, R. Soc. Open Sci. 4 (2017) 160975.
[60] M.X. Ma Ben, Zhang Yi, Huibo Chen, Qiang Wang, Li Lanhhua, Prediction of suitable habitats of Ixodes persulcatus in China, Chin J Schisto Control 33 (2) (2021).
[61] B.L. Stone, Y. Tourand, C.A. Brissette, Brave new worlds: the expanding universe of lyme disease, Vector Borne Zoonotic Dis. 17 (2017) 619–629.
[62] H. Tian, S. Zhou, L. Dong, T.P. Van Boeckel, Y. Cui, S.H. Newman, J.Y. Takekawa, D.J. Prosser, X. Xiao, Y. Wu, et al., Avian influenza H5N1 viral and bird migration networks in Asia, Proc. Natl. Acad. Sci. U. S. A. 112 (2015) 172–177.
[63] A. Keskin, K.A. Erciyas-Yavuz, Preliminary investigation on ticks (Acari: ixodidae) infesting birds in kızılırmak delta, Turkey, J. Med. Entomol. 53 (2016) 217–220.
[64] J. Chen, J. He, R. Bergquist, Challenges and response to pandemics as seen in a One Health perspective, Science in One Health 1 (2022) 100010.
[65] X.-N. Zhou, M. Tanner, Science in One Health: a new journal with a new approach, Science in One Health 1 (2022) 100001.
[66] A. Inci, A. Yildirim, O. Duzlu, M. Doganay, S. Aksoy, Tick-borne diseases in Turkey: a review based on One Health perspective, PLoS Neglected Trop. Dis. 10 (2016) e0005021.
[67] Z.H. Sun, E.Y. Wan, Y.L. Agbana, Y. Zhang, X.N. Zhou, K. Kassegne, Global One Health index for zoonoses: A performance assessment in 160 countries and territories, iScience 27 (2024) 109297.